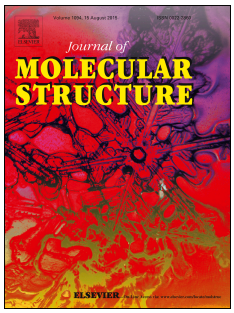

Crystal structures, Hirshfeld surface analysis and PIXEL calculations of four (*E*)-1-(2-hydroxyphenyl)-3-phenylprop-2-en-1-one derivatives, containing methoxy substituents. The importance of π interactions

Ligia R. Gomes, John N. Low, Alan B. Turner, James L. Wardell, Alessandra C. Pinheiro

PII: S0022-2860(20)30977-7

DOI: https://doi.org/10.1016/j.molstruc.2020.128652

Reference: MOLSTR 128652

To appear in: *Journal of Molecular Structure*

Received Date: 27 February 2020

Revised Date: 5 June 2020

Accepted Date: 8 June 2020

Please cite this article as: L.R. Gomes, J.N. Low, A.B. Turner, J.L. Wardell, A.C. Pinheiro, Crystal structures, Hirshfeld surface analysis and PIXEL calculations of four (*E*)-1-(2-hydroxyphenyl)-3-phenylprop-2-en-1-one derivatives, containing methoxy substituents. The importance of π interactions, *Journal of Molecular Structure* (2020), doi: https://doi.org/10.1016/j.molstruc.2020.128652.

Author	Roles
Ligia R. Gomes	Hirshfeld surface and PIXEL calculations
John N. Low	Principal crystallographer
James L. Wardell,	Diagrams, second crystallograpraher, writer, supervisor
Alessandra C. Pinheiro	Synthesis and characterisations
Alan B Turner	Original ideas: Initial study

Crystal structures, Hirshfeld surface analysis and Pixel calculations of four (*E*)-1-(2-hydroxyphenyl)-3-phenylprop-2-en-1-one derivatives, containing methoxy substituents. The importance of π interactions, by Gomes, Low, Turner, Wardell, Pinheiro

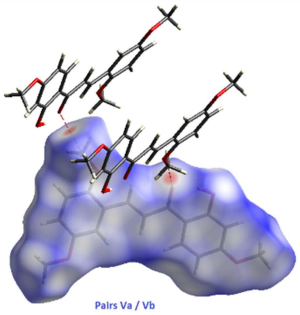

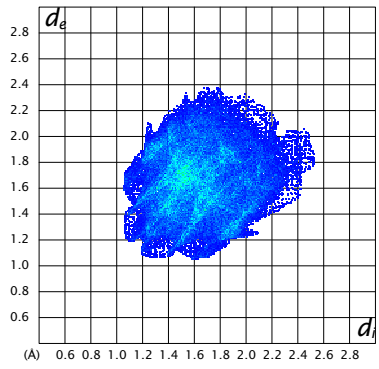

Crystal structures, Hirshfeld surface analysis and PIXEL calculations of four (*E*)-1-(2-hydroxyphenyl)-3-phenylprop-2-en-1-one derivatives, containing methoxy substituents. The importance of π interactions.

Ligia R. Gomes[1,2], John N. Low[3], Alan B. Turner,[3ǂ] James L. Wardell,[3,4*] Alessandra C. Pinheiro[4]

[1] FP-ENAS-Faculdade de Ciências de Saúde, Escola Superior de Saúde da UFP, Universidade Fernando Pessoa, Rua Carlos da Maia, 296, P-4200-150 Porto, Portugal,

[2] REQUIMTE, Departamento de Química e Bioquímica, Faculdade de Ciências da Universidade do Porto, Rua do Campo Alegre, 687, P-4169-007, Porto, Portugal,

[3] Department of Chemistry, University of Aberdeen, Meston Walk, Old Aberdeen, AB24 3UE, Scotland,

[4] Instituto de Tecnologia em Fármacos e Farmanguinhos, Fundação Oswaldo Cruz, 21041-250 Rio de Janeiro, RJ, Brazil.

ǂ Died: 16th February 2014

Abstract

A detailed structural analysis has been carried out on four chalcone (*E*)-1-(2-hydroxyphenyl)-3-phenylprop-2-en-1-one derivatives, having a varying number of methoxy substituents, namely (*E*)-3-(3,4-dimethoxyphenyl)-1-(2-hydroxyphenyl)prop-2-en-1-one, (**1**), (*E*)-3-(4-methoxyphenyl)-1-(2-hydroxy-4-methoxyphenyl)prop-2-en-1-one, **2**, (*E*)-3-(2,5-dimethoxyphenyl)-1-(2-hydroxy-4-methoxyphenyl)prop-2-en-1-one, **3**, and (*E*)-3-(2,5-dimethoxyphenyl)-1-(2-hydroxy-3,4-dimethoxyphenyl)prop-2-en-1-one, **4**. Crystal structures were determined at 100 K by single crystal X-ray diffraction. Compound **2** displayed an unexpectedly large interplanar angle of 25 and 28.°° between the phenyl groups in the two independent molecules, due to the formation of a dimeric substructure requiring a pronounced phenyl group rotation to minimise steric hindrance. Such a substructure was absent in **1**, **3** and **4**. In all cases the 2-hydroxyl substituent forms intramolecular hydrogen bonds with its neighbouring carbonyl group. Different combinations of C—H···O, C—H··π and/or π ··π interactions are displayed by **1**, **3** and **4**, with also C=O···π intermolecular interactions present in **2**. The relative contributions of various intermolecular contacts in these structures were investigated using Hirshfeld surfave analysis and the associated two dimensional fringerprint plots. Important molecule pairs were identified in the crystal structures using the PIXEL method. The PIXEL lattice energy calculations revealed that in all cases the dispersion contribution was the major contributor to the packing stabilization, followed by the Coulombic contribution.

A search of structures of alkoxy derivatives of (*E*)-1-(2-hydroxyphenyl)-3-phenylprop-2-en-1-one derivatives in the CCDC data base has also been carried out.

Keywords: chalcones; X-ray crystallography; Hirshfeld surface analysis; PIXEL calculations

1.Introduction

Chalcones form a well-studied chemical group having a 1,3-diaryl-2-propen-1-one framework, see Fig 1. The large number of known chalcone derivatives [reported to be more than 92,000 in August 2016] [1], stem both from their abundance in nature, especially in plants,their uses and their ready syntheses. Much of the study of chalcones, both man-made and natural compounds, has centred on their wide-ranging uses as biological agents [1-6], with over 1000 compounds reported in August 2016 to have some biological activity. However their potential utility extends beyond biological uses and includes such areas as optical materials [7-11]. Specifically, 2-hydroxychalcones, 2-HO-phenyl-C(O)-CH=CH-aryl, are very important precursors of flavonoids and related compounds[12,13] and have interesting high reactivity and optical properties in the excited state [14,15].

Well-established preparative routes to chalcones are available, paramount among these is the Claisen-Schmidt condensation [16,17], which utilizes the acid or base catalysed condensation of an aldehyde or ketone having an alpha-hydrogen with an aromatic carbonyl compound lacking an alpha hydrogen under homogeneous conditions [5], as illustrated in Scheme 1. The Claisen-Schmidt condensation has been well used in the almost 140 years since the initial reports of the condensation, with various modifications having been subsequently derived, including the use of ultrasound irradiation [18] and heterogeneous catalysts [19].

The crystal structures of various chalcones have been reported. Indeed over 3000 were listed in a very recent search of the CCDC data base on April 2019, with over 200 structures of these being for 2-HO-phenyl-C(O)-CH=CH-phenyl compounds [20]. Generally these 2-HO-phenyl-C(O)-CH=CH-aryl compounds possess intramolecular hydrogen bonding involving the 2-HO and the neighbouring carbonyl group.

We wish to report a study of the crystal structures, determined from data collected at 100K, Hirshfeld surfaces and PIXEL calculations of a series of four 2-HO-phenyl-C(O)-CH=CH-phenyl compounds. Related crystal structures, Hirshfeld surfaces and PIXEL calculations have been carried out on thione compounds [21,22]

Compounds investigated in our study are (*E*)-3-(3,.4-dimethoxyphenyl-1-(2-hydroxyphenyl)prop-2-en-1-one, (**1**), (*E*)-3-(4-methoxyphenyl-1-(2-hydroxy-4-methoxyphenyl)prop-2-en-1-one, **2**,(*E*)-3-(2,5-dimethoxyphenyl)-1-(2-hydroxy-4-methoxyphenyl)prop-2-en-1-one, **3**, and (*E*)-3-(2,5-dimethoxyphenyl)-1-(2-hydroxy-3,4-dimethoxyphenyl)prop-2-en-1-one, **4**, see Fig. 1. A previous determination of the crystal structure of **1** had been carried out from data collected at 100 K [23]: the same structure was

found in this study. However no Hirshfeld surface analysis nor PIXEL calculations had previously been carried out.

2.Experimental

2.1.General

Melting points were determined on a Griffin melting point apparatus and are uncorrected. Infrared spectra of samples, as neat powders, were recorded using a Perkin Elmer UART two, with ATR Diamond Cell, instrument. NMR spectra were recorded on a BrukerAvance 400 spectrometer in DMSO-d_6 at room temperature. Accurate mass measurements were determined using a Water Mass Spec. Model Xevo G2 QT of instrument and MassLynx version 4.1 software. Analytical thin layer chromatography (TLC) was performed on pre-coated silica gel 60 F254 aluminium plates with visualisation under UV light at 254 and 366 nm.

2.2.Synthesis

An aqueous solution of sodium hydroxide (30%, 8mL).was added with stirring to a solution of a substituted 2-hydroxyacetophenone (0.1 mol) and a substituted benzaldehyde (0.1 mol) in ethanol (20mL). The reaction mixture was stirred overnight at room temperature, by which time the reaction was shown to be complete by TLC. Ice-cold hydrochloric acid (10%, 30 mL) was added, and the solid product was collected, washed with ice-cold water (2x50 mL) and recrystallized twice from ethanol, see Scheme 1.

(*E*)-3-(3.4-Dimethoxyphenyl-1-(2-hydroxyphenyl)prop-2-en-1-one, 1, was prepared from 2-hydroxyacetophenone and 3,4-dimethoxybenzaldehyde, m.p.114-115^{o}C: lit. [24] m.p. 113–114 ^{o}C .

^{1}H NMR (DMSO-d_6): δ: 3.83 (3H, s, OCH_3), 3.88 (3H, s, OCH_3), 7.00(1H, d, J = 8 Hz), 7.02(1H, d, J = 8 Hz), 7.04(1H, d, J =8 Hz), 7.43 (1H, dd, J = 2 and 8 Hz), 7.57(2H, m), 7.83(1H, d, J = 12.2 Hz), 7.94 (1H, d, J = 12.2 Hz), 8.31, (1H, brd, J = ca 8 Hz), 12.80 (1H,s, OH).
^{13}C NMR (DMSO-d_6) δ: 55.63, 55.77, 110.93, 111.56,117.74, 118.79, 119.02, 120.50, 124.65,127.24, 130.77, 136.22, 145.69, 149.06, 151.72,162.14, 193.65.
HR-MS (ESI): m/z calcd. for $[C_{17}H_{16}O_4H]^+$ [M + H]+ 295.1135: found 295.1127.
(*E*)-3-(4-Methoxyphenyl-1-(2-hydroxy-4-methoxyphenyl)prop-2-en-1-one, 2, was prepared from 2-hydroxy-4-methoxyacetophenone and 4-methoxybenzaldehyde,
yellow needles, m.p. 114-116-^{o}C (EtOH); lit. [25] m.p 114.4-115.3 ^{o}C (EtOAc/hexane) .
^{1}H NMR (DMSO-d_6) δ: 3.84 (3H, s, OCH_3), 3.85 (3H, s, OCH_3), 6.51 (1H, d, J =1.5 Hz, aryl), 6.57 (1H, dd, J =1.3 and 8.4 Hz, aryl), 7.03 (2H, d =8.4 Hz, aryl), 7.82 (1H, d, = 12.2 Hz, olefinic), 7.89

(1H, d, J =12.2 Hz, olefinic), 7.89 (1H, d, J = 8.4 Hz, aryl), 8.28(1H, d, J =8.4 Hz, aryl), 13.61(1H, s, OH).

^{13}C NMR DMSO-d_6) δ: 55.40, 55.73, 100.92, 107.30, 113.83, 114.44,118.47, 127.19, 131.10, 132.54, 144.26, 161.57, 165.73, 165.85, 191.84.

HRMS: $[M+Na]^+$: found 307.0953. $C_{17}H_{16}NaNaO_4$ requires 307.0941; $[M+H]^+$: found 285.1133 $C1_7H_{17}O_4$ requires 285.1127.

(*E*)-3-(2,5-Dimethoxyphenyl)-1-(2-hydroxy-4-methoxyphenyl)prop-2-en-1-one, 3, was prepared from 2-hydroxy-4-methoxyacetophenone and 2,5- dimethoxybenzaldehyde as yellow needles, m.p. 107-109 ^{o}C; lit.[26] m.p. 108-111 ^{o}C.

^{1}H NMR (DMSO-d_6) δ: 3.81 (3H, s, OCH_3), 3.85 (3H, s, OCH_3), 6.52 (1H, d, J =2.0 Hz, aryl), 6.57 (1H, dd, J =2.0 and 8.0 Hz, aryl), 7.06 (2H, s, aryl), 7.60 (1H, s, aryl), 7.97 (1H, d, J =12.2 Hz, olefinic), 8.40 (1H, d, J =12.2 Hz, olefinic), 8.28 (1H, d, J =8.0 Hz, aryl), 13.51 (1H, s, OH).

^{13}C NMR DMSO-d_6) δ: 55.72, 55.75, 100.90, 107.44, 112.66, 113.08, 113.85, 118.53, 120.95, 123.30, 132.31,152.82, 153.31, 165.82, 165.98, 191.98.

HRMS: $[M+Na]^+$: found 337.1058. $C_{18}H_{18}NaO_5$ requires 337.1052

(*E*)-3-(2,5-Dimethoxyphenyl)-1-(2-hydroxy-3,4-dimethoxyphenyl)prop-2-en-1-one, (4), was prepared from 2-hydroxy-3,4-dimethoxyacetophenone and 2,5- dimethoxybenzaldehyde as yellow needles, m.p. 146-147^{o}C.

^{1}H NMR (DMSO-d_6) δ: 3.73 (3H, s, OCH_3), 3.81 (3H, s, OCH_3), 3.86 (3H, s, OCH_3), 3.92 (3H, s, OCH_3), 6.73 (1H, d, J = 8.0 Hz, aryl), 7.07 (1H, d, J = 1.0 Hz, aryl), 7.60 (1H, s), 7.98 (1H, d, J =12.2 Hz, olefinic), 8.13 (1H, d, J = 8.0Hz), 8.14 (1H, d, J =12.2 Hz, olefinic), 13.22 (1H,s, OH).

^{13}C NMR DMSO-d_6) δ: 55.72, 56.14, 56.17, 59.85, 103.63, 112,8, 113.07,115.20, 118.49, 121.02, 123.26, 127.36, 135.82, 138.48, 152.85, 157.85, 158.53,192.62.

HRMS: $[M+Na]^+$: found 367.1165. $C_{20}H_{16}NaO_6$ requires 367.1152

2.3. X-ray data collection and structure refinement.

All details are listed in Table 1 [27-33].

2.4.Lattice energy and intermolecular interaction energy calculations

Lattice energies and intermolecular interaction energies were calculated using PIXEL code implemented in the CLP package [34,35].The PIXEL program calculates intermolecular energies by distributed charge description on basis of a preliminary evaluation of charge density from

GAUSSIAN at MP2/6-311G** level of theory (CUBE option). The PIXEL mode calculates the total stabilization energies of the crystal packing, E_{tot}, distributed as Coulombic, (E_{coul}), polarization (E_{pol}), dispersion (E_{disp}) and repulsion (E_{rep}) terms between separate, rigid molecules. Coulombic terms are treated on the basis of coulombic law, polarization terms are calculated as a linear dipole approximation, dispersion terms are based on London's inverse six-power approximation involving ionisation potentials and polarizabilities and the repulsion term comes from a modulated function of the wave function overlap. The PIXEL calculations allows the identification of the pairs of molecules (motifs) which contribute most to the total energy of the packing.

2.5. Hirshfeld surface analyses

The Hirshfeld surfaces and two-dimensional Fingerprint (FP) plots [36] were generated using Crystal Explorer 3.1 [37]. The normalized contact distance, *d*norm, between -0.226 and 1.089, allows important regions to be identified, with d_{norm} being a symmetric function of distances to the surface from nuclei inside, d_i, and outside, d_e the Hirshfeld surface, relative to the appropriate van der Waal radii. Partitioning of the fingerprint plots were applied to identify and quantify the intermolecular interactions in the crystal lattice: the plots were decomposed to specify particular close contacts of pairs of atoms.

3. Results and discussion

3.1 General

Compounds were prepared by the general method shown in Scheme 1. Crystals used in the structure determination were grown by slow evaporation of solution**s** of the chalcone at room temperature in EtOAc for **1** and EtOH for **2-4.** Compound **1** crystallizes in the monoclinic space group, $P2_1/c$, $Z = 4$, compound **4** in the monoclinic space group, $P2_1/n$, with $Z = 4$, and **3** in the monoclinic space group I2/a with $Z = 8$, all with one molecule in the asymmetric unit. Compound **2** crystallizes in the triclinic space group P-1 with $Z = 4$ and with two independent molecules in the asymmetric unit.

3.2 Molecular conformations

The atom arrangements, numbering schemes and molecular conformations are shown for compounds **1**, **3** and **4** in Fig. 2 and for compound **2** in Fig. 3. In Fig. 3, the two independent molecules, A and B, of compound **2** are drawn linked by C113—H113···$O212_{(hydroxyl)}$ and C213—H213···$O112_{(hydroxyl)}$ hydrogen bonds: additionally an overlapping view of the two independent

molecules of **2** and a view of their spatial relationship are provided. The intramolecular hydrogen bonds are indicated as dashed lines. For compounds **1, 3** and **4** having one molecule in the asymmetric unit, the rings with carbon atoms C11 and C31 are referred to as rings A and B, respectively, while for compound **2**, having two independent chalcone molecules in the asymmetric unit, the rings with carbon atoms C111, C131, C121 and C231 are referred to as rings A, B, C and D, respectively.

Compounds **1**, **3** and **4** exhibit near planar arrangements, with angles between the two phenyl rings and the linker group [i.e. C_{11}-C_1(=O_1)-C_2=C_3-C_{31}] all less than 7^o, see Table 2. It is worth noting that compound **2**, despite having two methoxy substituents [one less than in the very near-planar compound **1**], exhibits sizeable interplanar angles between the linker unit and the phenyl ring B. This must be connected to the fact that the two independent molecules are linked, in the asymmetric unit, by C113—H113···$O212_{(hydroxyl)}$ and C213-H213···$O112_{(hydroxyl)}$ hydrogen bonds to form asymmetric dimers with small $R^2_2(8)$ rings [38], see Fig 3, and that the potential steric hindrance resulting from the *ortho* sited methoxy groups in phenyl rings B and D, is reduced on further rotation of the phenyl ring B and D out of the plane of the linker unit. As will be discussed below in the sections dealing with molecular pairs, other C—H···O intermolecularhydrogen bonds in compounds **1**-**4** do result in formation of other dimeric molecule pairs, however these sit comfortably with near planar molecules.

For all compounds, the interplanar angles between ring A / C and the linker and between the linker and ring B/D indicate progressive rotations in the same sense. Moreover, for each of the compounds in this study, the sum of these interplanar angles are very close to the interplanar angle between rings A and B. Interestingly the very similar rotations noted for the two independent molecules of **2** are in opposing directions, and hence the two molecules have a quasi-enantiomeric relationship, see Fig. 3.

The bond lengths in the linker unit are listed in Table 3. Similar values are found for the corresponding bonds in all four compounds. Delocalisation is apparent in the linker units on comparing the measured bond lengths with those expected for single and double bonds. Thus the compounds have an extended π system involving both phenyl rings and the linker unit, i.e. involving the complete molecules.

3.3 Crystal structures

The intermolecular interactions found in the group of compounds **1- 4** are π···π and C—H···π and C=O···π interactions, and C—H···O hydrogen bonds, with each compound having its own set of some or all of these interactions. The intermolecular interactions for each compound are listed in Table 4. Details of the most significant molecule pairs (motifs), including their symmetry operations, geometric parameters, and energies, are listed in Table 5. The calculated lattice energy for each compound **1**-**4** is shown in Table 6.

*3.3.1.Crystal packing of **1**.*

The intermolecular interactions in **1** are π···π and C—H···π interactions, and C—H···O hydrogen bonds, details are listed in Table 4. The six most stable molecule pairs / motifs, **I** to **VI**, are listed in order of decreasing energy in Table 5a. The most favoured molecular pair, motif **I**, see Fig. 4a, involves a $\pi_A \cdots \pi_A$ interaction, which concentrates very much on a localised C15···C15^{i} contact at 3.65 Å; symmetry code: i = -x,1-y, 1-z: the ring centroid---ring centroid distance is long at 4.5229(7) Å. In making this π-linked motif the most energetically favoured motif, a low E_{rep} value, 13.1 kJ/mol, compensates for the moderate E_{disp} value of -34.6 kJ/mol. Motif **II** is linked by a more complete $\pi_B \cdots \pi_B$ interaction, with a Cg···Cg separation of3.5824(6) Å. Combinations of this $\pi_B \cdots \pi_B$ interaction with C341—H34C···π_B interaction used, to generate motif **VI**, provides the column illustrated in Fig. 4b.

All the oxygen atoms participate in C—H···O hydrogen bonding. The combination of C3—H3···O33$_{(methoxy)}$ and C36—H36···O34$_{(methoxy)}$ hydrogen bonds, used in the linking of motif **IV**, generate C(5),C(5),$R^2_2(9)$ chains of molecules [38], see Fig. 4c: individually, the C3—H3···O33and C36—H36···O34 hydrogen bonds each produce C(5) chains. Motif **III** is generated from C16—H16···O12$_{(OH)}$ hydrogen bonds: these hydrogen bonds connect to form C(5) chains, see Fig. 4d. A fourth hydrogen bond, C35—H35···O1$_{(carbonyl)}$, is used to link motif **VI**: these hydrogen bonds generates zigzag C(8) chains, see Fig.4e.

Combination of all the molecule pairs results in a three dimensional structure. A crystal packing diagram for **1 is** shown in Fig. 5.

*3.3.2.Compound **2***

The intermolecular interactions in compound **2** are C—H···O hydrogen bonds, and C—H··π and C=O··π interactions, see Table 4. Compound **2** is the only one of the compounds reported here to exhibit C=O··π interactions. A search of the CCDC data base indicated that C=O··π interactions are present in less than 20% of (*E*)-1-(2-hydroxyphenyl)-3-phenylprop-2-en-1-one derivatives. Details of the nine most energetically favoured molecule pairs/motifs in compound **2** are displayed in Table 5b, while arrangements of molecules generated from specific combinations of the intermolecular interactions are illustrated in Fig.6. Due to there being two independent molecules, A and B, in the asymmetric unit, as shown in Fig. 3, the molecule pairs are grouped in three sections in Table 5b as: Mol A···Mol A (pairs**II** and **III**), Mol A···Mol B (pairs**I** and **IV** to **VII**) and Mol B···Mol B pairs (**VIII** to **IX**). The Mol A···Mol A pairs,**II** and **III**, are essentially equivalent to the Mol B···Mol B pairs,**V111** and **IX**, as corresponding close contacts are involved in forming corresponding pairs, but as shown in Table 5a, the energies can differ slightly between corresponding pairs due to the different molecular conformations of Mol A and Mol B, for example compare E_{tot}

values of -36.5 and -35.0 for **II** and **VIII**, and -26.8 and -23.6 kJ.mol^{-1} for **III** and **IX**. In the discussion which follows, rings with carbon atoms, C111, C131, C211 and C231, are designated rings with subscripts A, B, C and D, respectively.

Molecule pairs, **II** and **VII**, utilize C137—-H13C···O11$_{(carbonyl)}$ and C237—-H23B···O21$_{(carbonyl)}$ hydrogen bonds, respectively, to form symmetric dimers with $R^2_2(22)$ rings, and molecule pairs, **III** and **IX,** involve C115—H115···O134$_{(methoxy)}$ and C215—H215···O234$_{(methoxy)}$ hydrogen bonds, respectively, also to form symmetric dimers, but with $R^2_2(24)$ rings. These molecule pairs are imbedded in the partial sheet shown in Fig. 6a. The other molecule pair, linked by C—H···O hydrogen bonds is pair **V**, a Mol A···Mol B pair, and thus an unsymmetrical dmer, is formed from C213—-H213···O112 and C113—-H113···O112$_{(hydroxy)}$ hydrogen bonds and contains a $R^2_2(8)$ ring. This too is illustrated in Fig. 6a. The sheet shown in Fig 6a, formed from all C—-H···O hydrogen bonds present in compound **2**, is composed of a network of different rings, including a $R^6_6(26)$ ring, generated from all six hydrogen bonds, C215—-H215···O234$_{(methoxy)}$, C213—-H2135···O112$_{(hydroxy)}$), C137—-H13C···O11$_{(carbonyl)}$, C115—-H115···O134$_{(methoxy)}$, C237—-H23B···O21$_{(carbonyl)}$, C113—-H113···O212$_{(hydroxy)}$. The sheet is essentially planar as shown in Fig. 6b.

The motifs linked by π interactions are **I**, **IV**, **VI** and **V11**: of these, **I** and **IV**, are illustrated in Fig. 6c. Motif **I** has the molecules arranged as in the asymmetric unit. The arrangement in Fig. 6c can be considered as being constructed from single columns of molecules, whose alternate layers are linked (i) by C136—-H136···π_D and C21=O21···π_C (used in linking motif **I**) and (ii) by C133—-H133···πD, C132—-H132···π_D and C11=O11···π_C interactions (used in linking motif **IV**). The single column is linked by C113—-H113···O212$_{(hydroxy)}$ and C213—-H213···O112$_{(hydroxy)}$ hydrogen bonds (employed in the formation of motif **V**) to provide a two-molecule wide column: Fig. 6d provides another view of the non-planar arrangement shown in Fig. 5c. In the single column the molecules are all orientated in the same direction, which in each row of the double column, the molecules are linked head- to-head. The two other π-linked motifs, which are not illustrated in Fig. 6c, are **VI** and **VII**: the interactions, C235—-H235···π_B and C232—-H232···π_B, separately linking the molecules in motifs **VI** and **VII**, are shown in Fig.6e and form an alternating chain of molecules A and B.

The energy calculated for the Mol A···Mol A molecule pairs, **II** and **III**, sums to -63.3 kJmol^{-1}, while the sum from the equivalent Mol B···Mol B pairs, **VII** and **IX**, is slightly less at -58.6 kJmol$^{-1.}$

Four other molecule pairs, two Mol A···Mol A and two corresponding Mol B···Mol B pairs, with E_{tot} values between -15 and -10 kJ.mol^{-1}, were also indicated by the PIXEL calculations. None of these pairs exhibit direct close connections but used neighbouring molecules to act as conduits of the electronic interaction between the molecules in the molecule pair. The coordinates of the partner molecules to the reference molecule are *x, y, z* are *2-x, 1-y, -z* and *1-x,1-y, -z.*

Combination of all the molecule pairs results in a three dimensional structure. A crystal packing diagram for **2** is shown in Fig. 5.

*3.3.3.Compound **3***

The intermolecular interactions in **3** are $\pi\cdot\cdot\pi$ and C—H$\cdot\cdot\pi$ interactions and C—H$\cdots$O hydrogen bonds, details are listed in Table 4. Details of the seven most energetically favoured molecule pairs/motifs in compound **3** are displayed in Table 5c, while arrangements of molecules generated from specific combinations of the intermolecular interactions are illustrated in Fig. 7.

The three most energetically important motifs, **I** – **III**, can be seen within a cage-type arrangement generated from the $\pi_A\cdot\cdot\pi_A$ and $\pi_B\cdot\cdot\pi_B$ interactions, C141—H14A$\cdots$O35$^{i}_{(methoxy)}$ (symmetry code: *i*: 0.5-x,2.5-y,0.5-z) hydrogen bonds and H14A$\cdots$O35$^{ii}_{(methoxy)}$ contacts (symmetry operation: *ii*: 1-x,1-y,1-z), see Figs. 6a and b. To differentiate the different H14A$\cdots$O35contacts in the cage, the bond distances for H14A$\cdots$O35^{i} and H14A$\cdots$O35^{ii}, as calculated using the MERCURY program (2.385 and 2.912 Å, respectively) have been added to Fig. 7a.

The view looking down the cage is illustrated in Fig.7b and shows the formation of each rung of the cage from pairs of C141—H14A$\cdots$O35$^{i}_{(methoxy}$ hydrogen bonds, with each rung being a motif **II**, with a $R^2_2(28)$ ring. The red dots, at the centres, Cg, of each of the phenyl rings in Fig. 7b, indicate where the $\pi_A\cdot\cdot\pi_A$ and $\pi_B\cdot\cdot\pi_B$ interactions progress down through the cage, linking the rungs of the cage. These $\pi_A\cdot\cdot\pi_A$ and $\pi_B\cdot\cdot\pi_B$ interactions are the links for motif **I**, the most significant motif, see also Fig. 6c for a separate view of the π stacking arrangement, which has all molecules in the same orientation. The slippages in the $\pi_A\cdot\cdot\pi_A$ and $\pi_B\cdot\cdot\pi_B$ interactions are 1.647 and 1.872 Å, respectively, with the perpendicular distance between the phenyl rings of 3.5083(5) and 3.3932(5) Å, respectively, clearly point to the strength of motif **I**. The large $E_{(disp)}$ value of -87.3 kcal/mol confirms the importance of the π interactions in this motif, see Table 5c.

Further links between the rungs of the cage are formed from H14A$\cdots$O35$^{ii}_{(methoxy)}$ contacts, as utilized in motif **III**. These contacts are outside the sum of the sum of the contact radii for H and O (2.70 Å). However, while suggesting such linkages are likely to be weak, motifs with similar values outside the contact radii sum have been considered to be significant for other compounds [see e.g., 37]. While the H14A$\cdots$O35 separations in**II** (symmetry code i) and in **III** (symmetry code ii) are markedly different, at 2.39 and 2.91Å, respectively the E_{tot} values of **II** and **III** at -33.9 and -27.8 kcals/mol, respectively, are not too dissimilar. However, the distributions of the E_{Coul}, E_{pol}, E_{disp} and E_{rep} energy components are markedly different, being -26.8, -9.0, -34.1 and 35.9 for **II** and -4.3, -5.5, -40.9 and 22.8 kcal/mol for **III**, indicating that compensations between components are at play. The low E_{Coul}, value for **II** and the low E_{rep} value for **III a**re especially noticeable. The moderately high *Edisp* values for both **II** and **III** (-34.1 and -40.9 kJmol^{-1}), suggest that π interactions play a role in

the stabilization of both **II** and **III** - a consequence of their presence in a cage dependent on a considerable degree of π involvement.

The rungs in the cage arrangement, shown in Fig. 7b, are further linked by pairs of C231---H32B---$O32_{(methoxy)}$ hydrogen bonds into a chain of molecules: these hydrogen bonds form $R^2_2(6)$ rings (motif **IV**), see Fig.7d. Two C—H···O hydrogen bonds separately generate spiral chain of molecules. Thus, C32---H32B---$O1_{(carbonyl)}$ hydrogen bonds, which link motif **V**, form a spiral C(9) chain, propagated in the direction of the *b* axis, see Fig. 7e. In motif **V**, the H···O distance, at 2.69 Å is within the value (2.72 Å) of the sum of the contact radii of hydrogen and oxygen, however in motif (**VI**) (see Fig.7f), which is linked by C141—H14C···$O12_{(hydroxyl)}$ hydrogen bonds, the H···O distance, at 2.80Å, is somewhat outside this limit. The E_{tot} values for **IV** and **VI** are small at -15.6 and -14.6 kJmol^{-1}, respectively, with both having no dominant energy component. The C141—H14C···O12 hydrogen bonds generate spiral chain, also propagated down the *b* axis, but here with seven atom repeats, ie., C(7) chains. In both the C321—H32B···$O1_{(cabonyl)}$, and C141—H14C···$O12_{(hydroxyl}$ spiral chains, the molecules are linked in head-to-head manners, see Figs.7e and f. The last close contact to consider is a H35B···C33separation of 2.94 Å, just outside the sum of the corresponding atom contacts of 2.90Å, for hydrogen and carbon, which generates motif **V1**, see Fig. 7g. The E_{tot} value for motif **V1** is -15.4 kcal/mol with the highest contributor to the overall energy being E_{disp} (-20.4 kJ.mol^{-1}).

Combination of all the molecule pairs results in a three dimensional structure. A crystal packing diagram for **3 is** shown in Fig. 5.

*3.3.4.Compound **4***

The intermolecular interactions present in **4** are π··π and C—H··π interactions, and C—H···O hydrogen bonds, see Table 4 for details. Details of the six most energetically favoured molecule pairs/motifs in compound **4** are displayed in Table 5d, while arrangements of molecules generated from specific combinations of the intermolecular interactions are illustrated in Fig. 8.

The π_A··π_B interactions are involved in linking the most energetically favoured molecule pair, motif **I**. The high dispersion energy, E_{disp} = -109.4 kJ.mol^{-1}, attributed to this pair confirms the importance of the π··π interactions. The π_A··π_B dimers in combination with C33-H33---π_B interactions and C231---H32C---$O14_{(methoxy)}$ hydrogen bonds produce a sheet of molecules, see Fig. 8a, which includes both motifs **I** and **IV. T**he C33-H33---π_B interactions and C231---H32C---$O14_{(methoxy)}$ hydrogen bonds are involved in the contacts in motif **4**: the C231—H32C···$O14_{(methoxy)}$ hydrogen bonds on their own generate C(13) chains, with molecules linked in a head-to-tail fashion. The non-parallel molecules in the arrangement shown in Fig. 8a are at an angle of 48.8^o.

There are six oxygen atoms and all, except the O35 methoxy oxygen, partake in hydrogen bonding, which lead to the formation of molecule pairs, **II** to **V1**. Motif **II**, a dimer containing a

$R^2_2(14)$ ring [38], is formed from a pair of C36—H36···$O1_{(carbonyl)}$ hydrogen bonds: these dimers are linked into a chain by C141—H14A···$O13_{(methoxy)}$ and C141—H14A···$O14_{(methoxy)}$ hydrogen bonds, as shown in Fig. 8b. The C141—H14A···O13 and.C141—H14A···O14 hydrogen bonds are involved in the linking of motif **V**, which contains a three ring $R^1_2(5)$, $R^1_2(6)$, $R^1_2(5)$ system.

Molecule pair **III is** generated from C141—H14B···$O12_{(hydroxyl)}$ hydrogen bonds, which lie within a C(7) chain of molecules propagated in the direction of the *a* axis, see Fig. 8c. The molecule pair **VI** is linked by C131—H13A···$O32_{(methoxy)}$ hydrogen bonds, which generates a C(12) chain propagated in the direction of the *b* axis, see Fig. 8d.

Combination of all the intermolecular interactions provides a three dimensional structure of **4.** A crystal packing diagram for **4 is** shown in Fig. 5.

3.3.5. Lattice energies

The lattice energy values (Table 6) indicate that the dispersion energy, E_{disp}, is the major contributor towards the crystal stabilization, with progressive increases from -173.8 to -202.3 kJ.mol^{-1} from compounds **1** to **4**. The second highest contributor in each case was the Coulombic component, which ranged from-55.9 to -74.3 kJ.mol^{-1} for **1** -**4**. Confirmation of these findings was obtained from the intermolecular energy calculations for the identified molecular pairs (motifs) in Table 6.

3.3.6.Hirshfeld surface analysis

Hirshfeld surface analysis (HAS) has been carried out into the packing motifs and the contributions of the major intermolecular interactions to the crystalline structure. Figs. 9 -12 illustrate several views of the surfaces mapped over d_{norm} for compounds **1 - 4**, respectively, each of those views indicating red spots corresponding to atom…atom close contacts between the molecules placed at *x*, *y*, *z* with their partner molecule as defined in the motif lists in Table 5.

Views of the Hirshfeld surface for compound **1** are shown in Fig. 9: in Fig. 9a , the π···π stacking interaction, which links motif **II**, is indicated, in Figs. 9b-d O···H contacts involvedin motifs **III** – **V** are highlighted, and in Fig. 9e, the close contacts corresponding to the C341—H34···πB interactions are featured.

Fig. 10 shows four views of the Hirshfeld surface of molecules of compound **2**. In Figs. 10a-c the surfaces shown are of Mol A, while in Fig. 10d surfaces of both molecules A and B are shown. The red spots in Fig. 10a relate to the H···C closecontact corresponding to the C136— H136···πD interaction of motif **I** , which connects the two molecules as in the asymmetric unit. The red spots in Fig.10b-10c correspond to O···H close contacts defning motifs **II-V** and motif **IX**. Those contacts are identified in the figures. In a similar way Fig. 11 presents three views of the Hirshfeld surface of

compound **3**, showing red spots suggestive of C···O close contacts (identified in the figures) that define motifs **III** to **IV** (see Table 5c). Finally, Fig. 12 shows views of the Hirshfeld surface of compound **4**. The red spot areas in Fig. 12b and 12c relates to O···H close contacts (again identified in the figures) which define motifs **II** to **V**. Fig. 12a shows C···C contacts corresponding to those forming motif **I**.

.

3.3.7. FP Plots

The FP plots are depicted for all compounds in Fig. 13 as are the partial FP plots, indicating the individual contributions of the C···H/H···C, C···C and H···O/O···H close contacts. The spikes pointing towards the bottom left in the overall FP plots are due to O···H/H···O contacts. The percentage atom···atom contacts, shown in Table 7,were obtained by partial analysis of the FP plots. The highest percentage O···H/H···O contacts is shown by compound **3**. Compound **3** also exhibits the lowest H···C/C···H and highest C···C contacts. For all compounds, the highest atom···atom contacts are the H···H contacts.

It is of interest to note the percentages of close atom···atom contacts for the two independent molecules of compound **2** in Table 7. As mentioned above, the two independent molecules of **2** have a quasi-enantiomeric relationship, and as shown in Table 10, both exhibit the same percentages of close atom···atom contacts.

4. Conclusion.

As with most (*E*)-1-(2-hydroxyphenyl)-3-phenylprop-2-en-1-one derivatives, compounds **1, 2** and **4** are very near planar; compound **2** exhibits a greater deviation from planarity due to steric hindrance experienced on dimerization. The intermolecular interactions experienced among the four compounds are π···π, C—H···π and C=O···π interactions and C—H···O hydrogen bonds, the latter just for compound **2**. The most energetically stable motifs for compounds **1**, **3** and **4** were linked by π···π interactions, but for **2** (the least planar molecule), the two most favoured motifs were linked by C—H···O hydrogen bonds to provide symmetric Mol A andMol B dimers. For all of the molecules, the PIXEL lattice energy calculations revealed that the dispersion contribution was the major contributor to the packing stabilization, followed by the Coulombic contribution. The percentage of H···O/H···O contacts varied from the highest, 29.0for **3,** to the lowest, 21.8 in each of the independent molecules of **2**. The percentage of H···C/C···H contacts were ca.28for compounds **1** and **2,** but below 20 for compounds **3** and **4**. Compound **3** also exhibits the highest C···C contacts. For all compounds, the highest atom···atom contacts arethe H···H contacts.

.

5. Survey of (*E*)-1-(2-hydroxyphenyl)-3-phenylprop-2-en-1-one derivatives, having methoxy substituents and related published compounds.

As shown by a search of the CCDC data base, the majority of alkoxy derivatives of (*E*)-1-(2-hydroxyphenyl)-3-phenylprop-2-en-1-one derivatives reported in the literature are methoxy derivatives, with only a few having other alkoxy groups. For all the alkoxy derivatives, the structures are formed from some, or all, of C—H···O hydrogen bonds, C=O··π, C—H··π and π··π interactions, with the C=O··π interaction appearing less frequently. Details from the literature search of the interplanar angles, involving the phenyl groups and the linker group between the phenyl groups, are shown in Table 8 and the Supplementary Table 1: a few additional compounds with hydroxyl groups and other alkoxy groups are included in these tables for reference purposes. The interplanar angles in these tables are listed in the order Ph_A··· linker, linker···Ph_B and Ph_A···Ph_B, and also when there are two independent molecules in the asymmetric unit Ph_C··· linker, linker···Ph_D and Ph_C···Ph_D. In the following, the interplanar angles discussed are the angles between the two phenyl rings, i.e., Ph_A···Ph_B and Ph_C···Ph_D angles.

Two sections in Table 8 list changes in the interplanar angles and intermolecular interactions in methoxy substituted (*E*)-1-(2-hydroxyphenyl)-3-phenylprop-2-en-1-one derivatives on varying the substituents in one phenyl ring while keeping the other phenyl ring constant. The Supplementary Table 1 lists data for the remaining methoxy derivatives found in the search. The recent survey of the crystal structures of compounds with methoxy substituents clearly illustrates that the vast majority of compounds possess angles between phenyl groups smaller than 16^o, unless steric hindrance plays a role. Of course, any significant steric effect will change matters, but the fact that the vast majority of these methoxy derivatives exhibit small interplanar angles shows that steric efforts are generally not of great import for these methoxy derivatives.

Large deviations from planarity arise when there are multi and especially adjacent substituents present, as in (*E*)-1-(4,6-dihydroxy-2,3-dimethoxyphenyl)-3-phenylprop-2-en-1-one [39]: [CCDC code: MEBBEB], (*E*)-1-(2-hydroxy-3,4-dimethoxyphenyl)-3-(4-hydroxyphenyl)-2-propen-1-one [40] [CCDC code: SANZOX] and 2′-hydroxy-4,4′,5′,6′-tetramethoxychalcone [41]: [CCDC code:KASGIV], entry numbers 19, 23 and 25, respectively in Table 8. Alternatively, serious deviations from planarity can arise, even from relatively simple and non-bulky compounds, bearing few substituent, on particular associations in the crystal e.g., as shown by (*E*)-3-(4-methoxyphenyl-1-(2-hydroxy-4-methoxyphenyl)prop-2-en-1-one, **2**,[this study]. The large interplanar angle (ca 29 ^{o}) found in the relatively simple compound, (*E*)-1-(2-hydroxyphenyl)-3-(2-methoxyphenyl)-2-propen-1-one, [42] [CCDC code: LIKDEO], entry number 7, in Table 8, with only one methoxy substituent, albeit in an *ortho* site in ring B, is unexpectedly high. It is apparent that the influence of

substituents on interplanar angles is complex, for example compare the angles found in compounds with a methoxy group *ortho* to the linker group in ring : 3.53(7) in LOVDOR [43 [entry no 12, Supplementary Table 1], 5.30(11) in VAZGUY [44] [entry no 14, Supplementary Table 1], 13.64(11) in CIQFOZ [45] [entry 9, Supplementary Table 1], 15.22(8) in SAPCAO [46] [entry 10, Table 8], 15.38(6) in compound **3**, [this study], 16.39(10) in AYOZUK [47] [entry 9, Table 8], 28.84(9) in LIKDEO [42] [entry 7, Table 8], and 29.60(9) in UYATEV [48] [entry no 8, Table 8. Such variations do not have simple explanations

The small interplanar angles in the straight-chained alkoxy substituted compounds, 2-HOC_6H_4-CO-CH=CH-C_6H_4OR-4 (R = Me) [CCDC code: XIGQEK01] [49], (R = Et) [CCDC code: SUZPIN] [50], (R = n-C_6H_{13}) [CCDC code: SOYPEC] [51] and (R = n-$C_{10}H_{21}$), [CCDC code: VOQNEV] [52], entries 2 - 5, respectively, in Table 8, contrasts with the much larger angle for the compound with R = n-$C_{12}H_{25}$ [CCDC code: MOSYEZ] [53], entry 6 in Table 8, and provides a further example of the difficulty of rationalising the planarity of many of these compounds.

It is noticeable in Tables 3, 8 and Supplementary Table 1, that, in many cases, the successive rotations of the linker and ring B out of the plane of the ring A occur in the same sense.

Finally, it is noticeable that for such a well-studied family of compounds, whose structures are built from a small number of weaker C—H···O hydrogen bonds, C=O··π, C—H··π and π··π interactions, there are few, if any, known polymorphs.

Supplementary material

Supplementary Table 1 and full details of the crystal structure determinations in cif format are available in the online version, at doi: xxxxxxxx. The cif-files have also been deposited with the Cambridge Crystallographic Data Centre with deposition numbers, 1913906, 1915360, 1917236 and 1917588, for compounds **1-4**, respectively, copies of which can be obtained free of charge on written application to CCDC, 12 Union Road, Cambridge, CB2 1EZ, UK (fax: +44 1223 336033); on request by e-mail to deposit@ccdc.cam.ac.uk or by access to http://www.ccdc.cam.ac.uk.

Acknowledgments: The use of the NCS crystallographic service at Southampton and the valuable assistance of the staff there are gratefully acknowledged. LRG thanks FCT [Fundação êpara a Ciência e a Tecnologia(UID/ Multi/04546/2013].

References

[1] C. Zhuang, W. Zhang, C. Sheng, W. Zhang, C. Xing, Z. Miao, Chem. Rev. 117 (2017) 7762.
[2] A. Rani, A. Anand, K. Kumar, V. Kumar, Expert Opin.Drug.Disc. 14 (2019) 249.
[3] D. K. Mahapatra, S.K. Bharti, V. Asati, , Eur. J. Med. Chem. 98 (2015) 69.
[4] P. Singh, A. Anand, V Kumar, Eur. J. Med. Chem. 85 (2014) 758.

[5] S. L.Gaonkar, U. N. Vignesh, Res. Chem. Intermed. 43 (2017) 6043.
[6] C. Capelini, V. R. F. Câmara, J. D. Figueroa Villar, J. M. C. Barbosa, K. Salomão, S. L. de Castro, P. Sales, S. M. F. Murta, T. B. Couto, M. C. S. Lourenço, J. L. Wardell, J. N. Low, E. F. da Silva, S. A. Carvalho, 2020, 16 : doi: 10.2174/1573406416666200121105215
[7] H. C. Kwong, M. S. Rakesh, C S. C. Kumar, S. R. Maidur, P. S. Patil, C. K. Quah, Y. F. Win, C. Parlak, S. Chandraju, Z. Kristallogr. 233 (2018) 349.
[8] V. Renuka, B. K. Revathi, D. R. Jonathan, M. K. Priya, P. S. Asirvatham, J. Mol. Struct. 1176 (2019) 838.
[9] D. A. Zainuri, M. Abdullah, S. Arshad, M. S. Abd Aziz, G. Krishnan, H. Bakhtiar, Optical Materials 86 (2018) 32.
[10] P. P. Vinaya, A.N . Prabhu, K. S. Bhat, V. Upadhyaya, J. Phys. Chem. Solids. 123 (2018) 300.
[11] S. Omar, M. Shkir, S. AlFaify, V. Ganesh, H. Algarni, P. S.Nayab, M. Arora, Opt.Quant.Electron. 50 (20180 50, 278.
[12] B. A. Bohm, Introduction to Flavonoids, Vol.2. Chemistry and Biochemistry of Organic Natural Products, Harwood Academic Publishers: Amsterdam, 1998.
[13] E. Grotewold, Ed.; The Science of Flavonoids; Springer, New York, 2006; ISBN 978-0-387-28822-2.
[14] I. E. Serdiuk, M. Wera, A. D. Rosha, , J. Phys. Chem. A 122 (2018) 2030.
[15] M. Dommett, R. Crespo-Otero, Phys. Chem. Chem. Phys. 19 (2017) 2409.
[16] L. Claisen, A. Claparède, Ber. Deutshen Chem. Gesellschaft. 14 (1881) 2460.
[17] J. G. Schmidt, Ber Deutschen Chem. Gesellschaft. 14 (1881) 1459.
[18] E. T. da Silva, L. S. da S. Pinto, S. M. S. V. Wardell, J. L. Wardell, M. V. N. de Souza, Lett. Org Chem. 16 (2019) 128.
[19] E. Rafiee, S. Eavani, Curr. Org. Chem. 21 (2017) 752.
[20] C. R. Groom, I. J. Bruno, M. P. Lightfoot, S. C. Ward, Acta Crystallogr. B72 (2016) 171.
[21] A. Saeed, Z. Ashraf, H. Nadeem, J. Simpson, H. Pérez, M. F. Erben, J. Mol. Struct. 1195 (2019) 796.
[22] A. Saeed, U. Flörke, A. Fantoni, A. Khurshid, H.Pérez, M. F. Erben, CrystEngComm. 19 (2017) 1495.
[23] J. P. Jasinski, R. J. Butcher, V. M. Khaleel, B. K. Sarojini, H. S. Yathirajan, Acta Crystallogr. E67 (2011) o845.
[24] M. J. Menezes, S. Manjrekar, V. Pai, R. E. Patre, S. G. Tilve, Ind. J. Chem. 2009, B48, 1311.
[25] K. Sugamoto, Y.-I. Matsusita, K. Matsui, C. Kurogi, T. Matsui, Tetrahedron 67 (2011) 5346.
[26] Y. K. Rao, S.-H. Fang, Y.-M. Tzeng, Biorg. Med. Chem. 12 (2004) 2679.
[27] CrysAlis PRO 1.171.40.47a, Rigaku Oxford Diffraction, 2017.
[28] P. McArdle, K. Gilligan, D. Cunningham, R. Dark, M. Mahon, CrystEngComm 6 (2004) 303.
[29] G.M. Sheldrick, Acta Crystallogr. A71 (2015) 3.
[30] C.B. Hübschle, G.M. Sheldrick, B. Dittrich, J. Appl. Crystallogr. 44 (2011) 1281.
[31] G.M. Sheldrick, Acta Crystallogr. C71 (2015) 3.
[32] C. F. Macrae, I. Sovago, S. J. Cottrell, P. T. A. Galek, P. McCabe, E. Pidcock, M. Platings, G. P. Shields, J. S. Stevens, M. Towler, P. A. Wood, J. Appl. Crystalllogr. 53, (2020) 226.
[33] A.L. Spek, Acta Crystallogr. D65 (2009) 148.
[34] A. Gavezzotti, J. Phys.Chem. B107 (2003) 2344.
[35] A. Gavezzotti, Mol.Phys.106 (2008) 1473.
[36] M. A. Spackman, J. J. McKinnon, D. Jayatilaka, CrystEngComm 10 (2008) 377
[37] M. J. Turner, J. J. McKinnon, S. K. Wolff, D. J. Grimwood, P. R. Spackman, D. Jayatilaka, M. A. Spackman, CrystalExplorer17, University of Western Australia, Australia, 2017.
[38] J. Bernstein, R. E. Davis, L. Shimoni, N. L. Chang, Angew. Chem. Int. Ed. Engl. 34 (1995) 1555.
[39] H. Usman, M.N. Jalaluddin, E.H. Hakim, Y.M. Syah, B.M. Yamin, Acta Crystallogr. 62E (2006) o209.
[40] J.R. Krishna, N.J. Kumar, M. Krishnaiah, C.V. Rao, Y.K. Rao, V.G. Puranik, Acta

Crystallogr.: 61E (2005) o1323
[41] P. Wafo, H. Hussain, S.F. Kouam, B.T. Ngadjui, U. Florke, K. Krohn, Acta Crystallogr. 61E (2005) o3017.
[42] J.-C. Wallet, E. Molins, C. Miravitlles, Acta Crystallogr. 51C (1995) 123.
[43] M. N.Akhtar, N. M. Sakeh, S. Zareen, S. Gul, K. M. Lo, Z. Ul-Haq, S. A. A. Shah, S. Ahmad, J. Mol. Struct.,1085 (2015) 97
[44] C.O. Miles, L. Main, B.K. Nicholson, Aust. J. Chem. 42 (1989) 1103,
[45] D. Koh, Acta Crystallogr. 69E (2013) o1809.
[46] H. Wu, Z. Xu, Y.-M. Liang, Acta Crystallogr. 61E (2005) o1434
[47] H.-K. Fun, T. Suwunwong, K. Chanawanno, P. Wisitsak, S.Chantrapromma, Acta Crystallogr. 67E (2011) o2287,
[48] D. Koh, IUCrData, 2016, 1, x161492, DOI: 10.1107/S2414314616014929
[49] B.K.Sarojini, H.S.Yathirajan, K. Mustafa, H. Sarfraz, M. Bolte, Acta Crystallog. 63E (2007) o4477,
[50] J. Horkaew, S. Chantrapromma, N. Saewan, H.-K. Fun, Acta Crystallogr. 66E (2010) o2346,
[51] Z. Ngaini, S.M.H. Fadzillah, H. Hussain, I.A. Razak, H.-K.Fun, Acta Crystallogr. 65E (2009) o1301.:
[52] Z. Ngaini, N.I.A. Rahman, H. Hussain, I.A. Razak, H.-K. Fun, Acta Crystallogr.65E (2009) o889.
[53] I.A. Razak, H.-K. Fun, Z. Ngaini, S.M.H. Fadzillah, H. Hussain, Acta Crystallogr.65E (2009) o1133

Highlights

1	The determination of the crystal structures of four chalcone derivatives
2	Study of the Hirshfeld surfaces of four chalcone derivatives
3	PIXEL calculations on four chalcone derivatives
4	Identification of the important molecular pairs in crystalline chalcone derivatives
5	Data base search of structures of (*E*)-1-(2-hydroxyphenyl)-3-phenylprop-2-en-1-one derivatives, containing methoxy substituents.

Declaration of interests

☐ The authors declare that we have no known competing financial interests or personal relationships that could have appeared to influence the work reported in this paper.

☐The authors declare that we have no financial interests/personal relationships which may be considered as potential competing interests.

Jim Wardell, on behalf of all the authors